

Investigation by optical techniques of the soot load non-uniformity in a premixed ethylene-air “flat” flame produced by a McKenna burner

Francesca Migliorini, Silvana De Iuliis, Francesco Cignoli and Giorgio Zizak

CNR-IENI, Sez. di Milano, via Cozzi 53, 20125 Milano

ABSTRACT

The McKenna burner was developed in the past in order to produce “flat” flames with wide regions of homogeneous composition and temperature. The premixed flames generated by this burner are monodimensional and the variation of chemical composition depends upon the reaction time (height above the burner surface). Owing to the characteristics of the flame produced by this burner, it was used to develop several optical diagnostic techniques for combustion studies. The radial uniformity is also assumed to be valid for very rich premixed flames stabilized by a stagnation plate placed few centimeters above the burner surface and in literature many papers can be found describing studies performed in heavily sooty flames.

During some measurements of soot volume fraction in rich premixed ethylene-air flames produced by a stainless steel McKenna burner it was observed that the soot distribution was far from being a flat one. This finding was in contradiction with the above mentioned assumptions. Several measurements have been performed by utilizing different optical techniques such as laser extinction and scattering (LES), mono-dimensional imaging of the scattering, laser-induced incandescence (LII) and laser-induced fluorescence (LIF) techniques. All measurements confirm a radial structure of the soot volume fraction. Soot is located preferentially around an annular region and is almost absent along the axis. Moreover the flame structure is sensitive to small variation in the flow field, indicating that all the experimental details must be carefully checked. These observations cast doubts about the conclusions obtained in several studies regarding the soot formation mechanisms.

INTRODUCTION

The McKenna burner was developed in the past in order to produce “flat” flames with wide regions of homogeneous composition and temperature [1]. This burner is produced by Holthuis & Associated (Sebastopol, CA) [2] and can be purchased in different versions. Figure 1 shows the basic version of the burner. The inner main body consists of a porous sintered plug of 60 mm diameter with a coil embodied in it for water cooling. A secondary porous bronze ring of 6 mm width is used for shielding the flame. The outer body is made of stainless steel with a diameter of 120 mm. The porous plug for the flame production can be made of bronze or stainless steel.

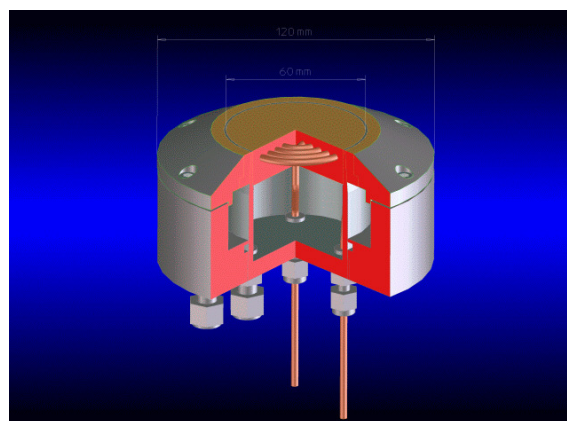


Figure 1: The McKenna burner

Due to the design the premixed flames generated by this burner are considered to be monodimensional with variation of chemical composition and temperature depending upon the reaction time (i.e. the height above the burner surface). Many studies have been performed by introducing probes axially within the flames for temperature and gas-chromatography measurements. Owing to the characteristics of the flame produced by this burner, it was used to develop several optical diagnostic techniques for combustion studies [3, 4]. Recently the burner was proposed as support for flames to be considered as temperature and species concentration standard [5]. The uniformity of temperature and chemical composition along a diameter of the flame was verified by Coherent Anti-Stokes Raman Scattering technique for H₂/air premixed flames with stoichiometry in the range from lean to slightly rich (up to $\Phi = 1.3$) [6]. This uniformity is also assumed to be valid for very rich premixed flames stabilized by a stagnation plate placed few cm above the burner surface and in literature many papers can be found describing studies performed in heavily sooty flames [7-9].

During some studies devoted to the comparison between gravimetric sampling and optical measurements of the soot load in rich premixed ethylene-air flames we observed that the radial distribution of soot volume fraction was far from being "flat". This finding was in contradiction with the above mentioned assumptions. Different optical techniques, such as laser extinction and scattering (LES), mono-dimensional imaging of the scattering and laser-induced incandescence (LII) techniques have been used to investigate the soot distribution. Laser-induced fluorescence (LIF) technique was also used to gain more information about the flame structure. All measurements confirm some dissymmetry and a radial structure of the soot volume fraction. In this work the results of these investigations are described. The observations here reported cast doubts about the conclusions obtained in several studies regarding the soot formation mechanisms.

EXPERIMENTAL APPARATUS

For these investigations a stainless steel porous plug was used for producing ethylene-air rich premixed flames. A stainless steel plate of 60 mm in diameter was placed at 20 mm height from the burner surface for flame stabilization. Mass flow meters (Bronkhorst, AK Ruurlo, The Netherlands) were used for controlling the flow of ethylene, air and nitrogen. The burner was placed on a motorized XYZ table in order to investigate the flame both in the axial and radial directions. Several flames were investigated. In this work we report only results obtained for a flame with the flow rates of C₂H₄ 1.35 l/min and air 7 l/min. This flame corresponds to a stoichiometry of $\Phi = 2.76$ with a C/O ratio of 0.92. The flow of nitrogen (used to shield the flame from surrounding air) was 15 l/min.

As mentioned, different optical techniques were used, such as laser extinction, line-imaging of the scattering, laser-induced incandescence (LII) and laser-induced fluorescence (LIF). These techniques are here only briefly described. Extinction measurements were performed with the red line ($\lambda = 647$ nm) of an Ar⁺Kr⁺ cw laser (Coherent Innova 70C). The laser beam was chopped by a mechanical chopper and mildly focused on the axis of the flame and the transmitted radiation was directed, by means of a two-lens system, at the entrance of a small integrating sphere and measured with a photo-sensor (Hamamatsu H5783-01). The signal was processed by a digital lock-in amplifier (Stanford, SR850 DSP). Each signal resulted from an average over 300 samples.

The line-imaging of the scattering was performed by using two lines of the same Ar⁺Kr⁺ cw laser (514 and 647 nm) sent separately across the flame. The scattered radiation was collected in the form of a picture of the flame crossed by the laser beam. The image was obtained using a cassegrain objective (Nikon, 500 focal length) and a CCD camera (PCO Pixelfly, 12 bit). Two interference filters (514 nm $\Delta\lambda = 9$ nm, and 647 nm $\Delta\lambda = 10$ nm), placed in front of the CCD camera, were used alternatively to detect the scattering signal. The images were processed by Image Pro Plus and MATHCAD software.

Laser-induced incandescence technique was performed by using the fundamental beam (1064 nm, 7 ns FWHM) of a Nd:YAG laser (Quanta System, SYL 202) operating at 6 Hz. The laser was steered onto a diaphragm (aperture 3 mm). A selected portion of the beam was imaged (magnification 1:1) on the flame axis. The uniformity of the probe cross section was checked with a webcam [10]. The incandescence signal was collected by a two mirrors system and focused on the entrance slit (2 mm height) of a small monochromator (JY H20) coupled with a fast photomultiplier (Hamamatsu R955, 1.5 ns rise time). The incandescence time decay curve was revealed at 450 nm with a fast digital oscilloscope (Tektronix, 1 GHz, 5 Gs/sec) optically triggered by the laser shot. Signal were stored in a PC and processed with MATHCAD.

Laser-induced fluorescence technique was applied by using three excitation wavelengths (488, 514 and 647 nm) of the Ar⁺Kr⁺ cw laser and collecting the LIF signals with a quartz optical fiber coupled with a spectrograph equipped with an intensified diode array detector (Tracor Northern TN-1710). A polarizer was placed just in front of the optical fiber in order to select the vertically polarized component of the emitted radiation.

RESULTS AND DISCUSSION

Figure 2 shows the axial profile of the mean soot volume fraction, f_v , as obtained with extinction measurements using the 647 nm laser line. Measurements obtained with shorter wavelengths can be influenced by absorption of gaseous species [11]. Different symbols refer to measurements performed in different days and show the reproducibility of the raw data. These results are obtained by considering the line-of-sight nature of the extinction measurements and ratioing the transmitted light intensity to the length of the flame as measured by the line imaging of the light scattering, as described later on.

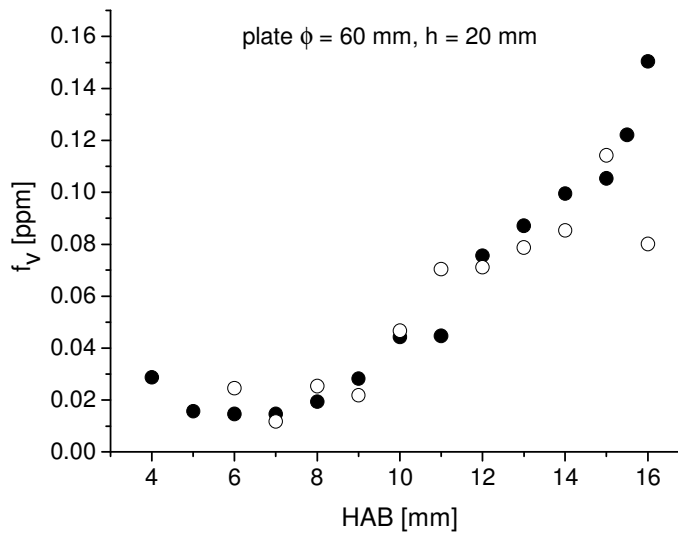


Figure 2. Mean soot volume fraction measurements on the axis obtained by extinction.

The soot concentration is very low in the first part of the flame and rapidly increases at about 8-9 mm above the burner surface. Measurements at heights close to 20 mm are very difficult to be obtained because the laser beam interferes with the stabilizing plate. The values reported in fig. 2 are in accordance with similar works reported in literature and are correct in the assumption of a “flat” soot distribution.

Lateral extinction measurements were also performed and, thanks to the assumed axial-symmetric geometry of the flame, were processed with an Abel inversion procedure in order to derive the radial extinction coefficient profile [12]. From the extinction coefficient the radial soot volume fraction can be obtained. Figure 3 shows the results (red dots). Surprisingly the profile is far from being “flat”. Soot is concentrated in an annular region with a strong minimum (practically no soot) on the axis. This unexpected result prompted to use another local technique for the investigation of soot distribution. The LII technique is well known to give measurements with a good spatial resolution. The LII intensity signals, proportional to the soot volume fraction, are reported in the same figure 3 as black dots. The two profiles compare well. The peaks of LII measurements are slightly shifted and the minimum is deeper on the axis. These differences can be attributed to a non perfect reproducibility of the flame. But these measurements, performed independently in different days, confirm that the soot distribution is not uniform.

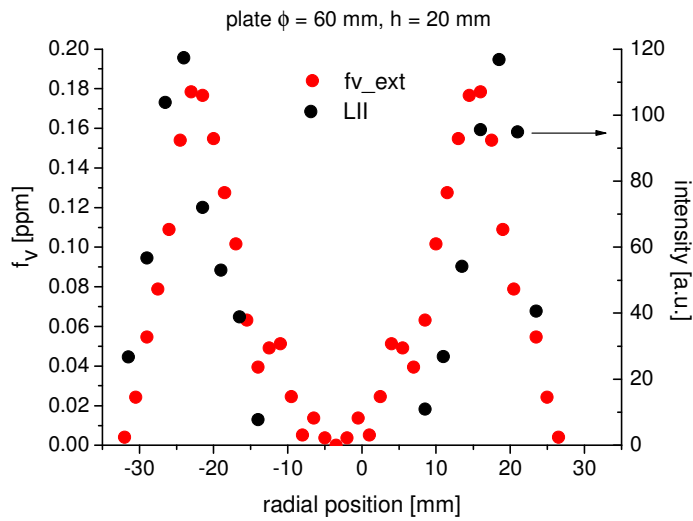


Figure 3. Comparison of soot volume fraction radial profiles obtained with extinction and LII techniques

Similar results were observed at different heights above the burner and in other experimental conditions such as using different flow rates and different stabilizing plates. This finding confirms that the observed annular structure is a general feature of the soot distribution of rich premixed flames produced by the stainless steel McKenna burner and is not an artifact due to some improper experimental arrangement.

As described in the experimental apparatus section, scattering measurements were carried out in the green and in the red spectral region. It is well known that scattering signal depends on the 6th power of the soot particle diameter, d_p , and, that, in conjunction with extinction, that depends on d_p^3 , allows to derive the particle size. Anyway line imaging of the scattering can give information about the soot distribution. In fact differences in intensity of the scattering signal can only be attributed to differences in soot size and particle number density. Figure 4 shows a typical image collected with the CCD camera, where the scattering from the 514 line of the laser, superimposed to the flame emission, is visible.

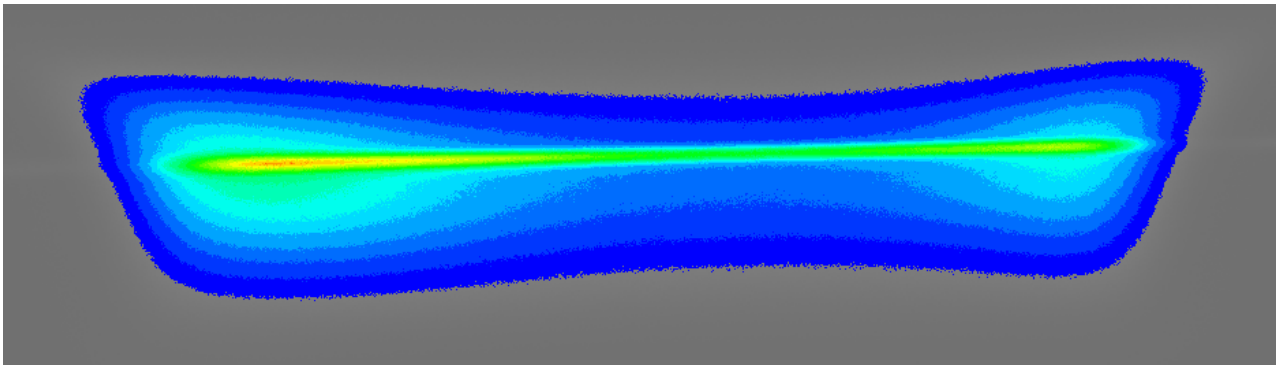


Figure 4. Line imaging of the scattering

The image shows that the scattering intensity is not uniform within the flame as well as the emission signal from the flame. In order to evaluate the contribution from the emission and from the scattering, a proper processing procedure was applied utilizing MATHCAD. Two sets of ten images, one with and the other without the laser, are collected to increase the signal-to-noise ratio. Each set was processed to produce average pictures which were then subtracted in order to obtain the scattering signal. Symmetrized scattering line-imaging measurements were performed at different heights

above the burner by using both the 514 nm and the 647 nm line of the laser. Strong differences are evident between the measurements. By using the 514 nm laser line scattering profiles are detected in the range of heights from 8 to 15 mm while with the 647 nm line the scattering signals can not be detected below 12 mm above the burner. The features of the curves are also quite different. Moving up in the flame the red (647 nm) scattering profiles show a structure with two external peaks and a minimum in the center, the green (514 nm) scattering, on the contrary, exhibit a quite flat profile across the flame with small peaks at 15 mm height. In figure 5 the comparison between results obtained by using the two lines at two different heights is shown.

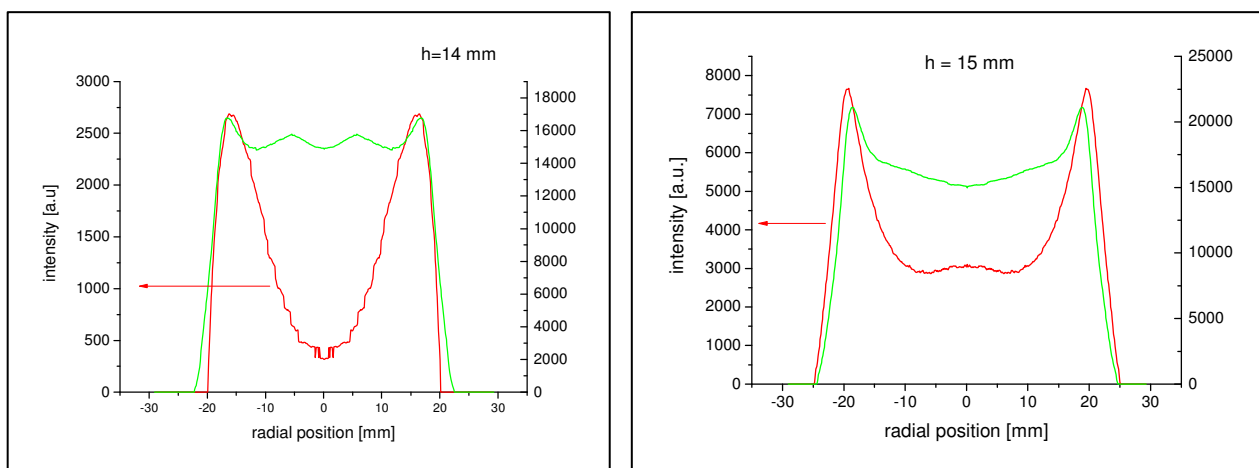


Figure 5. Scattering line imaging using the 514 nm (green) and 647 nm (red) line for two heights.

In particular the width of the flame is identical for both wavelengths indicating that in the external part of the flame only carbonaceous soot is present while in the core of the flame non-solid species contribute to the scattering signal in the green. These figures dramatically show that the flame structure is not radially uniform and different species are responsible for the scattering at the two wavelengths.

In order to discriminate the contribution of “non-solid” species to the scattering signal, laser-induced fluorescence was investigated at three excitation wavelengths (488, 514 and 647 nm) on the flame axis at 14 mm from the burner surface. Figure 6 shows the results.

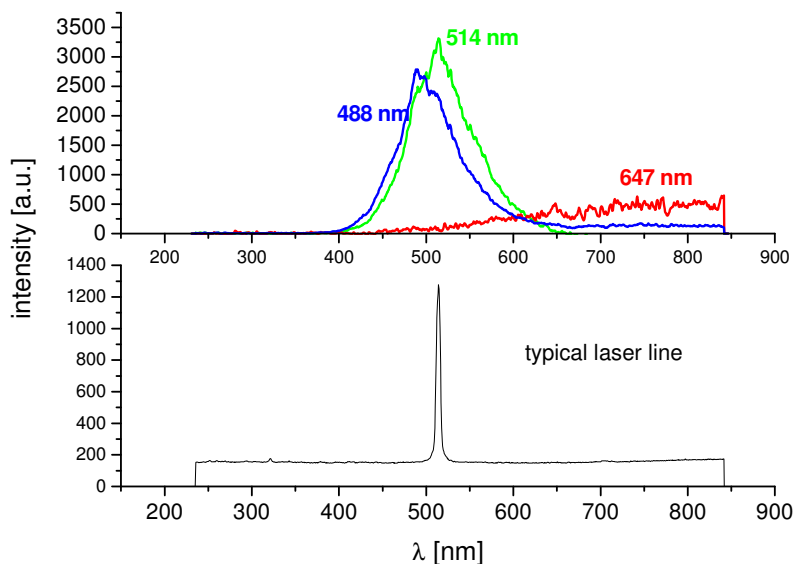


Figure 6: Laser-induced fluorescence of “non-solid” species on the axis (top), laser line (bottom).

The spectra excited with the 488 nm and 514 nm line present a similar band shape with the fluorescence band quite large and centered on the relative excitation wavelength. To give an idea of the spectral width used, the bottom of the figure shows the laser line at 514 nm as obtained from scattering by air. A different behavior is exhibited by the signal relative to the excitation at 647 nm, where no fluorescence is observed. Therefore the scattering signal in the red spectral region can be considered free from any fluorescence contribution and, consequently, can be related only to “solid or “mature” soot particles. For the other excitation wavelengths the fluorescence signal is quite significant in comparison to the resonant scattering. The scattering signal measured on the flame axis (see figures 4 and 5 left) is due to emission from “non-solid” and solid particles. Laser-induced fluorescence measurements were also performed at different heights on the axis, showing an increasing contribution from “non-solid” species with the height. These species could be related to the “nanoparticles of organic carbon” (NOC) as described in literature[13-14], although some spectral discrepancies are observed.

By comparing the results from the different techniques employed in this work, a quite complex structure of the rich flame produced by the stainless steel McKenna burner is revealed. In spite of the claimed “flat” structure, the flames are characterized by an annular distribution of soot particles (absorbing in the red and IR spectral regions). In the core of the flame “non-solid” species (absorbing and fluorescing in the visible) are present.

CONCLUSIONS

Several conclusions can be drawn by this work. Stainless steel McKenna burners are not completely reliable for obtaining stable “flat” axialsymmetric rich flames. Researches are suggested to verify the “flatness” of the flames investigated in their studies. Rich premixed flames exhibit an annular soot distribution with “non-solid” species on the axis. The use of short wavelength visible laser light for soot extinction/scattering measurements can result in significant errors due to presence of fluorescing species.

REFERENCES

1. D.W. Senser, J.S. Morse, V.A. Cundy, Rev. Sci. Instrum. **56** (6), 1279-1284 (1985).
2. www.flatflame.com.
3. S. Cheskis, Prog. Energy Combust. Sci. **25**, 233-252 (1999).
4. R.S. Barlow, C.D. Carter, Combust. Flame, **97**, 261-280 (1994).
5. G. Sutton, A. Levick, G. Edwards, D. Greenhalgh, Comb. Flame, **147**, 39-48 (2006).
6. S. Prucker, W. Meier, W. Stricker, Rev. Sci. Instrum., **65**, 2908-2911 (1994).
7. A. D'Alessio, G. Gambi, P. Minutolo, S. Russo, A. D'Anna, Proc. Combust. Inst. **25**, 645-651 (1994).
8. F. Xu, P.B. Sunderland, G.M. Faeth, Combust. Flame, **108**, 471-493 (1997).
9. B. Apicella, M. Alf , R. Barbella, A. Tregrossi, A. Ciajolo, Carbon, 1583-1589 (2004).
10. F. Cignoli, S. De Iuliis, G. Zizak, Appl. Spectrosc., **58**, 1372-1375 (2004).
11. G. Lo Castro, F. Migliorini, F. Cignoli, S. De Iuliis, G. Zizak, *XI Convegno Nazionale AIVELA*, Ancona 7-8 giugno 2005.
12. C.J. Dasch, Appl. Opt. **31**, 1146-1152 (1992).
13. P. Minutolo, G. Gambi, A. D'Alessio, S. Carlucci, Atmospheric Env. **33**, 2725-2732 (1999)
14. L.A. Sgro, G. Basile, A.C. Barone, A. D'Anna, P. Minatolo, A. Borghese, A. D'Alessio, Chemosphere **51**, 1079-1090 (2003).